

Novel Semisynthetic Betulinic Acid-Triazole Hybrids with In Vitro Antiproliferative Potential

Authors:

Gabriela Nistor, Alexandra Mioc, Marius Mioc, Mihaela Balan-Porcarasu, Roxana Ghiulai, Roxana Racoviceanu, ?tefana Avram, Alexandra Prodea, Alexandra Semenescu, Andreea Milan, Cristina Dehelean, Codru?a ?oica

Date Submitted: 2023-02-17

Keywords: betulinic acid-triazole derivatives, antiproliferative, cytotoxicity, melanoma, lung carcinoma, colorectal adenocarcinoma

Abstract:

Betulinic acid, BA, is a lupane derivative that has caught the interest of researchers due to the wide variety of pharmacological properties it exhibits towards tumor cells. Because of their prospective increased anti-proliferative efficacy and improved pharmacological profile, BA derivatives continue to be described in the scientific literature. The current work was conducted in order to determine the antiproliferative activity, under an in vitro environment of the newly developed 1,2,4-triazole derivatives of BA. The compounds and their reaction intermediates were tested on three cancer cell lines, namely RPMI-7951 human malignant melanoma, HT-29 colorectal adenocarcinoma, A549 lung carcinoma, and healthy cell line (HaCaT human keratinocytes). BA-triazole derivatives 4a and 4b revealed lower IC₅₀ values in almost all cases when compared to their precursors, exhibiting the highest cytotoxicity against the RPMI-7951 cell line (IC₅₀: 18.8 μ M for 4a and 20.7 μ M for 4b). Further biological assessment of these compounds executed on the most affected cell line revealed a mitochondrial level induced apoptotic mechanism where both compounds inhibited mitochondrial respiration in RPMI-7951 cells. Furthermore, the triazole-BA derivatives caused a significant decrease of the anti-apoptotic Bcl-2 gene expression, while increasing the pro-apoptotic BAX gene's expression.

Record Type: Published Article

Submitted To: LAPSE (Living Archive for Process Systems Engineering)

Citation (overall record, always the latest version):

LAPSE:2023.0160

Citation (this specific file, latest version):

LAPSE:2023.0160-1

Citation (this specific file, this version):








LAPSE:2023.0160-1v1

DOI of Published Version: <https://doi.org/10.3390/pr11010101>

License: Creative Commons Attribution 4.0 International (CC BY 4.0)

Article

Novel Semisynthetic Betulinic Acid–Triazole Hybrids with In Vitro Antiproliferative Potential

Gabriela Nistor^{1,2}, Alexandra Mioc^{2,3,*} , Marius Mioc^{1,2}, Mihaela Balan-Porcarasu⁴ , Roxana Ghiulai^{2,5}, Roxana Racoviceanu^{1,2} , Ștefana Avram^{2,6} , Alexandra Prodea^{1,2} , Alexandra Semenescu^{2,7} , Andreea Milan^{1,2} , Cristina Dehelean^{2,7} and Codruța Șoica^{2,5}

- ¹ Department of Pharmaceutical Chemistry, Faculty of Pharmacy, “Victor Babes” University of Medicine and Pharmacy Timisoara, Eftimie Murgu Square, No. 2, 300041 Timisoara, Romania
 - ² Research Centre for Pharmaco–Toxicological Evaluation, “Victor Babes” University of Medicine and Pharmacy, Eftimie Murgu Square, No. 2, 300041 Timisoara, Romania
 - ³ Department of Anatomy, Physiology, Pathophysiology, Faculty of Pharmacy, Victor Babes University of Medicine and Pharmacy, Eftimie Murgu Square, No. 2, 300041 Timisoara, Romania
 - ⁴ Institute of Macromolecular Chemistry ‘Petru Poni’, 700487 Iasi, Romania
 - ⁵ Department of Pharmacology–Pharmacotherapy, Victor Babes University of Medicine and Pharmacy, 2nd Eftimie Murgu Square, No. 2, 300041 Timisoara, Romania
 - ⁶ Department of Pharmacognosy, Faculty of Pharmacy, Victor Babes University of Medicine and Pharmacy, Eftimie Murgu Square, No. 2, 300041 Timisoara, Romania
 - ⁷ Department of Toxicology, Faculty of Pharmacy, “Victor Babes” University of Medicine and Pharmacy, Eftimie Murgu Square, No. 2, 300041 Timisoara, Romania
- * Correspondence: alexandra.mioc@umft.ro; Tel.: +40-256-494-604

Abstract: Betulinic acid, BA, is a lupane derivative that has caught the interest of researchers due to the wide variety of pharmacological properties it exhibits towards tumor cells. Because of their prospective increased anti–proliferative efficacy and improved pharmacological profile, BA derivatives continue to be described in the scientific literature. The current work was conducted in order to determine the antiproliferative activity, under an in vitro environment of the newly developed 1,2,4–triazole derivatives of BA. The compounds and their reaction intermediates were tested on three cancer cell lines, namely RPMI–7951 human malignant melanoma, HT–29 colorectal adenocarcinoma, A549 lung carcinoma, and healthy cell line (HaCaT human keratinocytes). BA–triazole derivatives 4a and 4b revealed lower IC₅₀ values in almost all cases when compared to their precursors, exhibiting the highest cytotoxicity against the RPMI–7951 cell line (IC₅₀: 18.8 μM for 4a and 20.7 μM for 4b). Further biological assessment of these compounds executed on the most affected cell line revealed a mitochondrial level induced apoptotic mechanism where both compounds inhibited mitochondrial respiration in RPMI–7951 cells. Furthermore, the triazole–BA derivatives caused a significant decrease of the anti–apoptotic Bcl–2 gene expression, while increasing the pro–apoptotic BAX gene’s expression.

Keywords: betulinic acid–triazole derivatives; antiproliferative; cytotoxicity; melanoma; lung carcinoma; colorectal adenocarcinoma



Citation: Nistor, G.; Mioc, A.; Mioc, M.; Balan-Porcarasu, M.; Ghiulai, R.; Racoviceanu, R.; Avram, Ș.; Prodea, A.; Semenescu, A.; Milan, A.; et al. Novel Semisynthetic Betulinic Acid–Triazole Hybrids with In Vitro Antiproliferative Potential. *Processes* **2023**, *11*, 101. <https://doi.org/10.3390/pr11010101>

Academic Editors: Alina Bora, Luminita Crisan and Sang-Jip Nam

Received: 19 November 2022

Revised: 23 December 2022

Accepted: 27 December 2022

Published: 29 December 2022



Copyright: © 2022 by the authors. Licensee MDPI, Basel, Switzerland. This article is an open access article distributed under the terms and conditions of the Creative Commons Attribution (CC BY) license (<https://creativecommons.org/licenses/by/4.0/>).

1. Introduction

Cancer chemotherapy has transformed cancer outcomes from terminal to treatable, or even curable; since its beginning, anticancer chemotherapy has evolved based on the continuous discovery in cancer cell biology so that today multitargeted therapy is being used [1]. However, the side effects of the anticancer drug therapy are often very severe, therefore the interests of oncologists have shifted from merely treating the tumor towards well–tolerated approaches [2]. Although belonging to traditional medicine, plant–derived compounds are currently recognized as reliable alternatives in the field of oncology considering their particular structures and mechanisms of action, which recommends them

as alternatives to avoid the limitations of conventional chemotherapy [3]. There are many classes of phytochemicals that have been used as such or served as scaffolds for the development of semisynthetic derivatives with antitumor properties or able to act as drug sensitizers.

Pentacyclic triterpenes are biologically active phytochemicals found in higher plants, exhibiting a huge plethora of biological effects that include anti-inflammatory and antitumor activities and containing lupane, oleanane, and ursane as the main scaffolds [4]. Betulinic acid is a lupane derivative which gained immense interest in the medical field not only due to its plethora of pharmacological effects but mainly due to its selective cytotoxicity against tumor cells; nonetheless, it demonstrates two major drawbacks: the low water solubility, which affects its bioavailability, and its insufficient supply from natural sources [5]. Therefore, the chemical modulation of various positions in betulinic acid, together with the development of new preparation methods from more abundantly found compounds such as botulin, have paved the way to achieve semisynthetic derivatives able to overcome the above-mentioned bottlenecks. The main molecular positions susceptible to modulation are the C₃, C₂₈ sites, ring A, as well as the C_{20–29} double bond; recent research emphasized that modifications on ring A and C_{20–29} double bond could significantly augment betulinic acid's biological effects (Figure 1) [6].

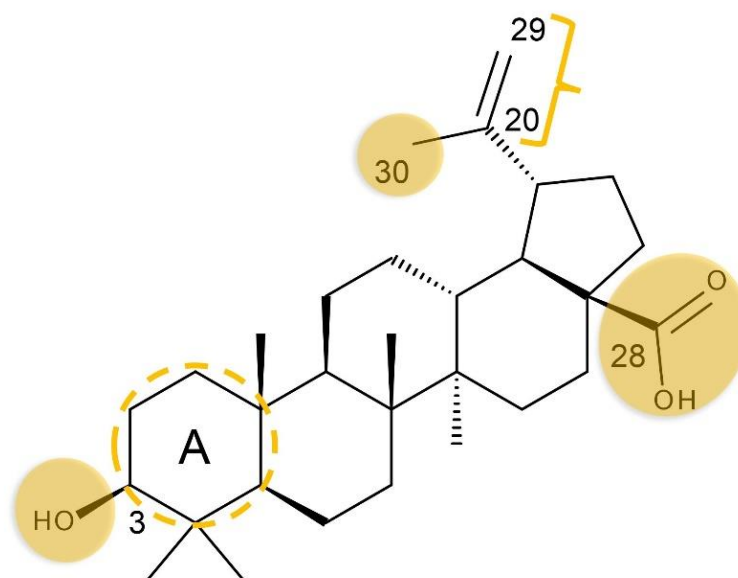


Figure 1. The main structural sites of betulinic acid susceptible to chemical modulation.

Among the many derivatization possibilities, the substitution with nitrogen-bearing heterocycles generates the most valuable agents within the medicinal chemistry; currently more than 75% of FDA approved marketed drugs bear nitrogen-containing heterocycles, while more such compounds will presumably soon reach the pharmaceutical market [7]. Such 1,2,3-triazole derivatives prepared from betulinic acid using click chemistry at C₃ were revealed as effective anti-leukemia agents with remarkably small IC₅₀ values (within the micromolar range), thus showing a 5–7 fold increased potency compared to the parent compound (Figure 2) [8].

Similar compounds were also synthesized by Shi et al. with compound 30–[4–(4–fluorophenyl)–1H–1,2,3–triazol–1–yl] betulinic acid showing the highest potency as revealed by the IC₅₀ value of 1.3 μM [9]. The Huisgen 1,3-cycloaddition was used to prepare 1,2,3-triazole derivatives at C₃₀ via the corresponding azides in the structure of betulinic acid, simultaneously conjugated at C₃; the most active derivatives revealed IC₅₀ values below 10 μM [10]. Functionalized triazole derivatives of betulinic acid were obtained by means of click cycloaddition through the modulation of the C₂₈–carboxyle group; the

study revealed two series of lead compounds as anticancer agents against murine breast cancer and human pancreatic cancer [11]. Sousa et al. published in 2019 a comprehensive review emphasizing the main chemical processes able to functionalize betulinic acid and several related compounds [12]; various modulations were applied starting from simple transformations and click chemistry reactions and reaching complex molecules such as heterocycle–fused derivatives and polymer conjugates.

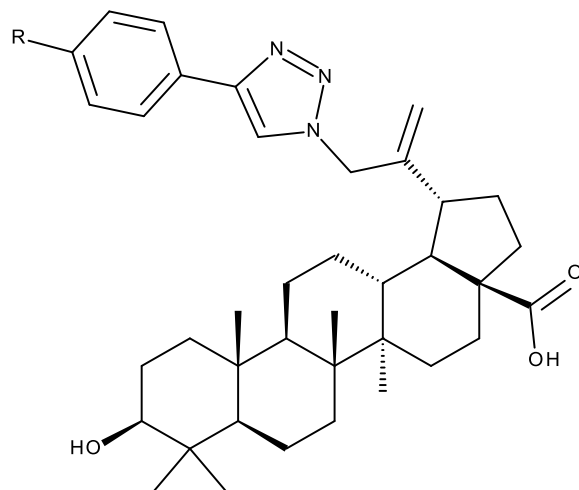


Figure 2. 1,2,3–triazole–substituted derivatives of BA acid synthesized via click chemistry acting as effective anti–leukemia agents.

The current study is a continuation of the previously published paper [13], which reported the cytotoxic activity of a C₃–acetylated 1,2,4–triazole derivative of BA; the compound revealed significant and selective cytotoxic effects against melanoma cells through mitochondrial apoptosis. Some studies reported that by inserting aryl groups as substituents in the triazole moiety grafted at C₃₀ it may increase the antitumor activity of the resulting compounds [9,10]; on the contrary, when modulating the carboxyl group at C₂₈, the cytotoxic activity increased with the increase of the molecule’s hydrophilic character imprinted partially by the triazole substituent. In order to clarify the impact of such C₃₀–substitutions on the compound’s cytotoxic activity, the current study aims to synthesize some derivatives of betulinic acid bearing the 1,2,4–triazole ring supplementary substituted with an aryl group by the chemical modulation of C₃₀, followed by their physicochemical characterization. Subsequently, the semisynthetic derivatives will be biologically tested in terms of cell viability; moreover, since their previously published triazole analogue revealed a pro–apoptotic activity, we aimed to identify the underlying anticancer mechanism by performing DAPI staining, respirometry studies and rt–PCR assay.

2. Results

2.1. Chemistry

The synthetic preparation, together with the reaction media necessary to obtain BA–triazole derivatives (**4a**, **4b**), are shown in Figure 3. Using modifications of previously reported methods [14,15], good yields (> 50%) were achieved for the triazole derivatives (**3a**, **3b**) and the brominated acetyl–BA (**2**). In comparison to earlier steps, the alkylation of the thiol group on the triazole structure (**3a**, **3b**) using BrBA in DMF/K₂CO₃ resulted in lower yields of BA–TZ derivatives (**4a**, **4b**). Although the precursors were rather pure, TLC analysis showed that the reaction resulted in at least two additional major compounds among the many lipophilic side products. Despite this, the chromatographic separation (chloroform:acetate 1:1 eluent) remained feasible due to the substantial R_f value differences. The structure of all synthesized compounds was validated through ¹H and ¹³C NMR

spectroscopy. All spectral data is available in the Supplementary Materials File uploaded with the present manuscript.

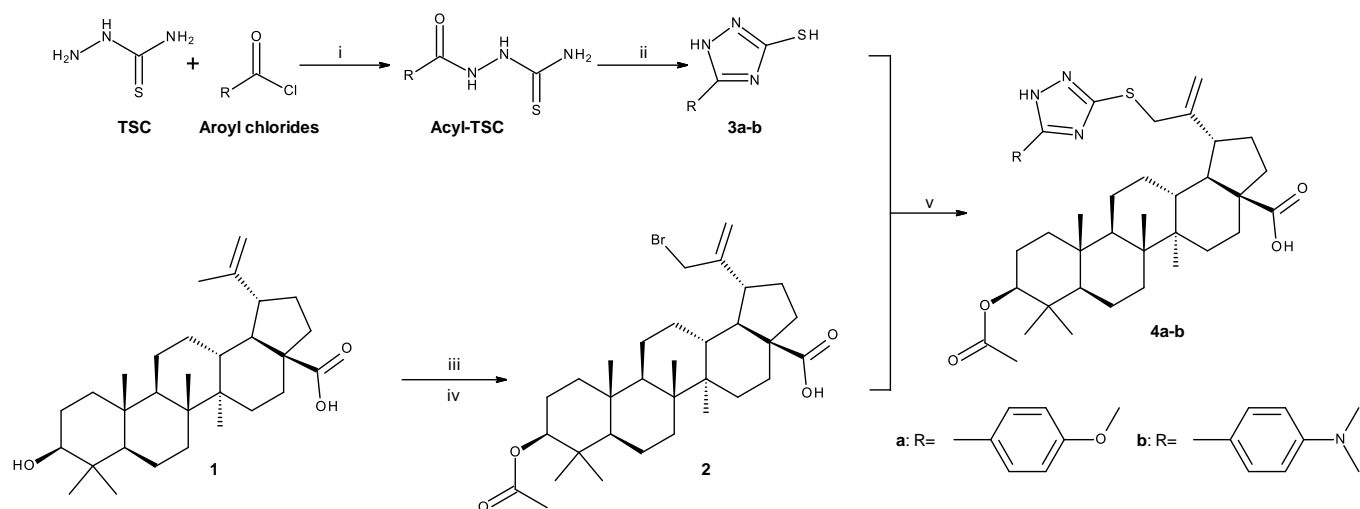


Figure 3. Synthesis pathways used to obtain BA–triazol derivatives; TSC = thiosemicarbazide, **1**—betulinic acid, **2**—3 β –O–Acetyl–30–bromo–betulinic acid, **3a**–5–(4–methoxyphenyl)–1H–1,2,4–triazole–3–thiol, **3b** – 5–[4–(dimethylamino)phenyl]–1H–1,2,4–triazole–3–thiol, **4a**–3 β –O–Acetyl–30–[5–(4–methoxyphenyl)–1H–1,2,4–triazol–3–ylsulfanyl]–betulinic acid, **4b**–3 β –O–Acetyl–30–[5–[4–(dimethylamino)phenyl]–1H–1,2,4–triazol–3–yl]sulfanyl]–betulinic acid; reaction conditions: i. pyridine/DMF, 1h, 50 °C; ii. H₂O, NaOH, reflux; iii. acetic anhydride, pyridine, DMAP, r.t, 12 h; iv. NBS, CCl₄, r.t, 48 h; v. DMF, K₂CO₃, r.t, 72 h.

2.2. BA Triazole Derivatives Decrease Cell Viability of Malignant Melanoma Cells

Following a 48 h treatment period, the effect of **4a**, **4b**, as well as their precursors (0.08, 0.4, 2, 10, and 50 μ M) in HaCaT healthy human keratinocytes, RPMI–7951 malignant melanoma, A549 lung carcinoma, and HT–29 colorectal adenocarcinoma cells was determined by employing the MTT assay, which enabled the calculation of IC₅₀ values (Table 1); the recorded viability in all tested cell lines is depicted in Figure 4. Among all the cell lines, malignant melanoma (RPMI–7951) proved to be the most sensitive toward the BA derivatives, in particular compound **4a**, which showed the maximum cytotoxic effect; thus, RPMI–7951 was chosen for further detailed study regarding the compounds **4a** and **4b** cytotoxic mechanism.

Table 1. IC₅₀ (μ M) values of **4a**, **4b**, and their intermediates against normal and cancer cell lines; compounds displaying IC₅₀ values above 50 μ M were considered not effective and, therefore, the specific values were not shown.

Compound	HaCaT	RPMI–7951	A549	HT–29
	IC ₅₀ (μ M/L) \pm SD			
1	>50	30.8 \pm 3.63	44.3 \pm 6.81	>50
2	>50	29.7 \pm 3.96	22.6 \pm 3.01	26.4 \pm 2.74
3a	>50	>50	>50	>50
3b	>50	>50	>50	>50
4a	>50	19.8 \pm 2.25	28.3 \pm 3.21	36.9 \pm 4.57
4b	>50	20.7 \pm 2.21	32.4 \pm 3.68	31.3 \pm 4.02
5FU	30.5 \pm 2.8	19.5 \pm 1.72	6.9 \pm 0.92	>50

Available literature data as well as our own previous experiments revealed that 0.5% DMSO did not affect cell viability [16,17]. Subsequently we used DMSO–stimulated cells

(at 0.5%) as negative control. All cytotoxic active compounds exhibited a dose dependent activity (Figure 4). The starting compound, BA (1), and its brominated derivative, compound 2, had a significant activity on all tested cancer cell lines except HT-29, where BA was not effective, while the starting triazoles 3a and 3b did not exhibit IC_{50} values under 50 μ M (Table 1). The BA-triazole derivatives (compounds 4a and 4b) displayed lower IC_{50} values against all tested cell lines, as opposed to their precursors, with one exception where compound 2 acted slightly stronger in HT-29 cells. Simultaneously, among all tested cell lines, 4a and 4b were the most effective against RPMI-7951 cells, exhibiting IC_{50} values of $19.8 \pm 2.25 \mu$ M and $20.7 \pm 2.21 \mu$ M, respectively. The cytotoxicity of compounds 4a and 4b was compared to the positive control 5-fluorouracil (5FU). While 5FU was inactive in A549 lung cancer cells, no compounds were revealed to surpass 5FU in HT-29 cells. However, in the case of RPMI-7951 melanoma cell line, compound 4a exhibited a similar IC_{50} (19.8μ M) value when compared to the positive control 5FU (19.5μ M). These results suggested a high cytotoxic effect of compounds 4a and 4b against the RPMI-7951 melanoma cell line.

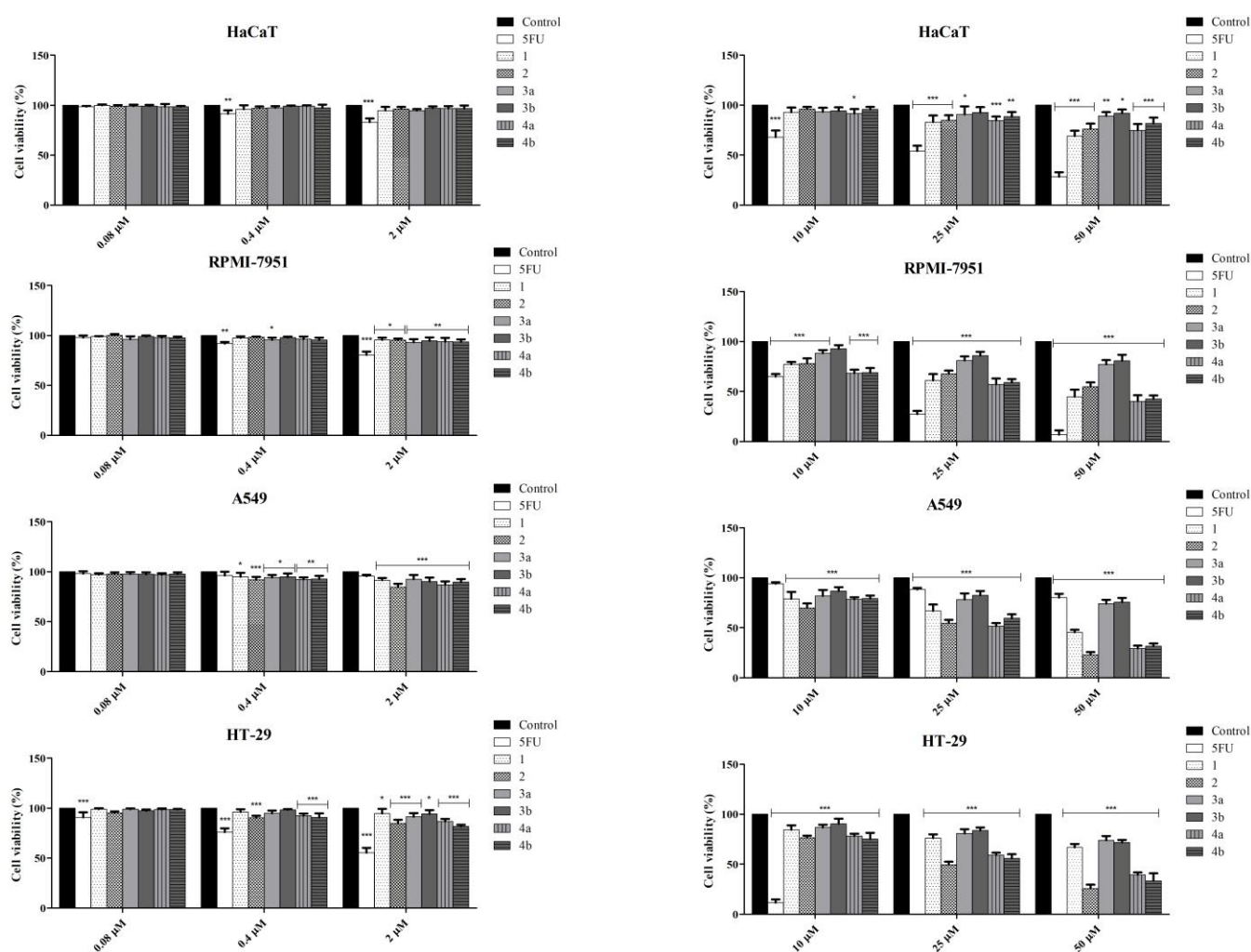


Figure 4. MTT assay assessed the cell viability of HaCaT, RPMI-7951, A549, and HT-29 cell lines after 48 h treatment with compounds 1-4b at 6 different concentrations. Negative control: untreated cells. Positive control: 5FU. All results are expressed as percentages in cell viability (%) taking negative control (DMSO-stimulated cells) as reference. All experiments were performed in triplicate and data are presented as mean values \pm SD. The statistical differences compared to negative control were identified through two-way ANOVA analysis followed by Bonferroni's multiple comparisons post-test (* $p < 0.05$, ** $p < 0.005$, and *** $p < 0.0001$).

2.3. BA Triazole Derivatives Induce Nuclear Alterations Associated with Apoptosis in Malignant Melanoma Cells

Considering the high antiproliferative effect at the lowest IC_{50} , the biological effects of compounds **4a** and **4b** were further investigated by assessing their effect on nuclear morphology using the DAPI staining. This particular dye that identifies nuclear modifications was employed, revealing that all tested compounds induced nuclei morphological changes, including shrinkage and fragmentation accompanied by the disruption of the cell membrane. All these changes were consistent with apoptotic processes; unlike necrotic processes where the nuclei stay relatively intact, in apoptosis the nucleus undergoes early degeneration and its morphological changes can be used as indicators of programmed cell death [18]. The morphological alterations in various degrees are presented by the yellow arrows in Figure 5, demonstrating changes that were consistent with apoptotic cell death, while apoptotic signs were not present on normal human keratinocytes (HaCaT).

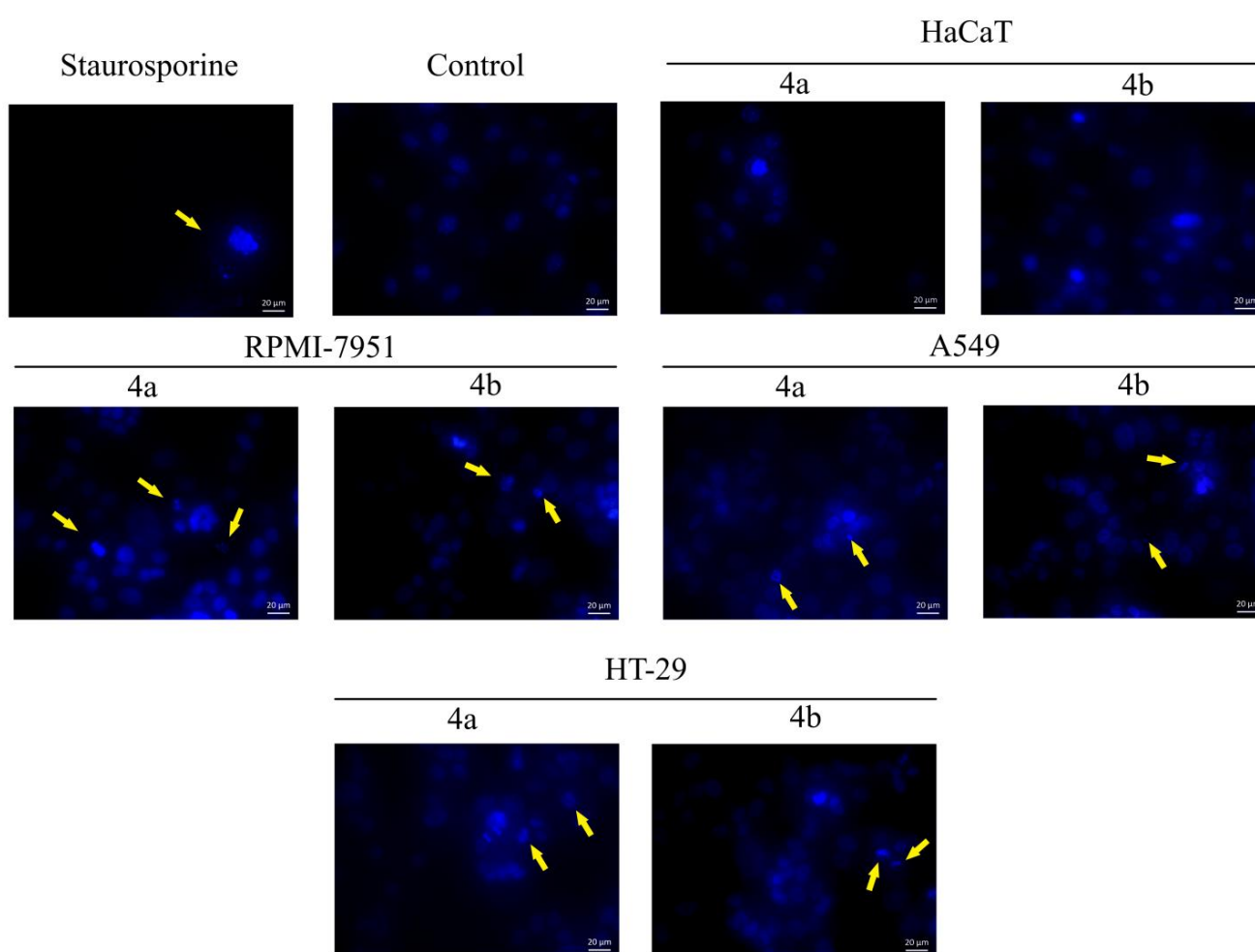


Figure 5. Morphological observation of HaCaT, RPMI–7951, A549, and HT–29 cell lines using DAPI assay, following treatment with **4a** and **4b** (tested at their respective IC_{50}) for 48 h. Positive control for nuclei apoptotic changes: staurosporine (5 μ M). The apoptotic morphological changes are indicated by yellow arrows.

2.4. Compounds **4a** and **4b** Influence the Expression of Anti–Apoptotic (*Bcl–2*) and Pro–Apoptotic (*BAX*) Genes

In order to investigate the apoptotic activity of compounds **4a** and **4b** in RPMI–7951 melanoma cells, the gene expression fold change of *Bcl–2* and *BAX* was assessed by using the quantitative real–time PCR method. Measurements were conducted after a 48 h

incubation period with the tested compounds. The compounds were tested at 18.8 μM and 20.7 μM , respectively, with values that induced a 50% reduction in RPMI–7951 melanoma cell viability. The results revealed that both compounds caused the upregulation of BAX gene expression vs. control (Figure 6) thus indicating a pro–apoptotic effect. Specifically, the highest effect was observed for compound **4a** (3.892), followed by compound **4b** (2.594) vs. control (1). Upon evaluating the relative fold change expression in Bcl–2 mRNA, compound **4a** determined the strongest decrease (0.275), while compound **4b** decreased only to 0.505 vs. control (1) (Figure 5).

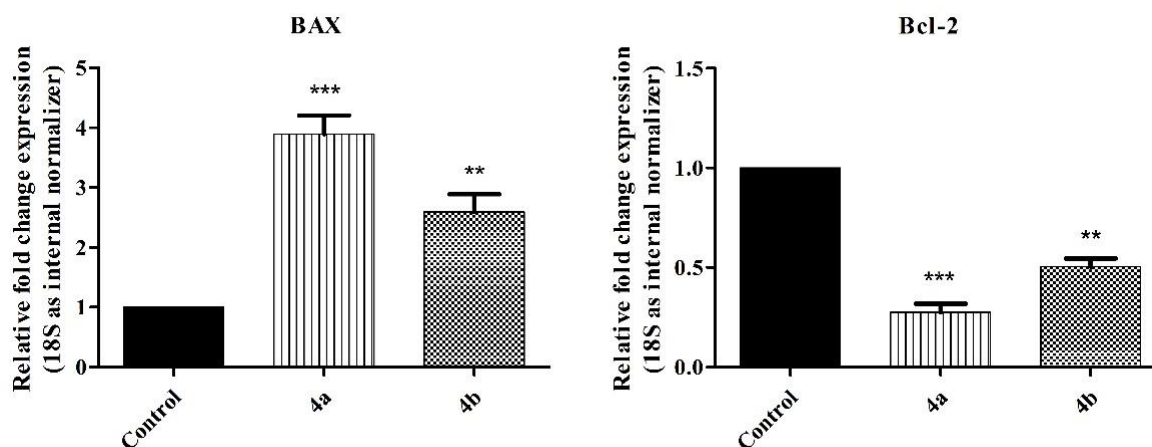


Figure 6. The difference in Bcl–2 and BAX mRNA expressions in RPMI–7951 cells following treatment with **4a** and **4b** (tested at IC_{50} : 18.8 μM and IC_{50} : 20.7 μM) for 48 h. The fold change expressions were compared to 18S RNA, while DMSO acted as the control. All experiments were performed in triplicate and the results were reported as mean values \pm SD. Statistical differences vs. DMSO stimulated cells were determined using one–way ANOVA with Dunnett’s post–test (** $p < 0.01$ and *** $p < 0.001$).

2.5. BA Triazole Derivatives Disrupt Mitochondrial Function of Melanoma Cells

The evaluation of mitochondrial function after the treatment with **4a** and **4b** at their IC_{50} values revealed the inhibition of mitochondrial respiration of RPMI–7951 cells, while normal HaCaT cells’ mitochondrial respiration remained unaffected (Figures 7 and 8). As presented in Figure 7, treatment of normal HaCaT cells with either compound did not affect the mitochondrial respiration. The expanded SUI technique was performed to permeabilized HaCaT as well as RPMI–7951 cells; mitochondrial respiratory rates assessed at 37 $^{\circ}\text{C}$ demonstrated that all chemicals can severely impair RPMI–7951 mitochondrial activity (Figure 8), while having no evident effect on HaCaT mitochondria. In particular, one mitochondrial parameter reduced by semisynthetic derivatives was routine respiration, which was solely dependent on endogenous ADP. Later, digitonine was used to permeabilize the cell membrane in order to assess the expanded OXPHOS (oxidative phosphorylation) and enable the molecular transit between external environment and cytoplasm. Following that, both basal and LEAK respiration was dramatically reduced, suggesting that the compounds may reduce the basal respiration. Tested at 18.8 μM (the IC_{50} value for **4a**) and 20.7 μM (the IC_{50} value for **4b**), the compounds considerably suppressed the OXPHOS respiration reliant on glutamate and malate substrates for complex I (OXPHOSCI) and the OXPHOS when succinate, a complex II substrate, was added (OXPHOSCI + II). The electron transport system’s maximum respiratory capacity in the complete noncoupled state (ETSCI + II) could be measured by quantifying the uncoupled state via FCCP titration. Compounds **4a** and **4b** were able to decrease the ETSCI + II and ETSCII, thus suggesting that they might lower the electron transport pathway capacity and impair ATP production. The mean values of the respiratory rates [pmol/(s \times mL)] obtained after the treatment of RPMI–7951 cells with compounds **4a** and **4b** are presented in Table 2.

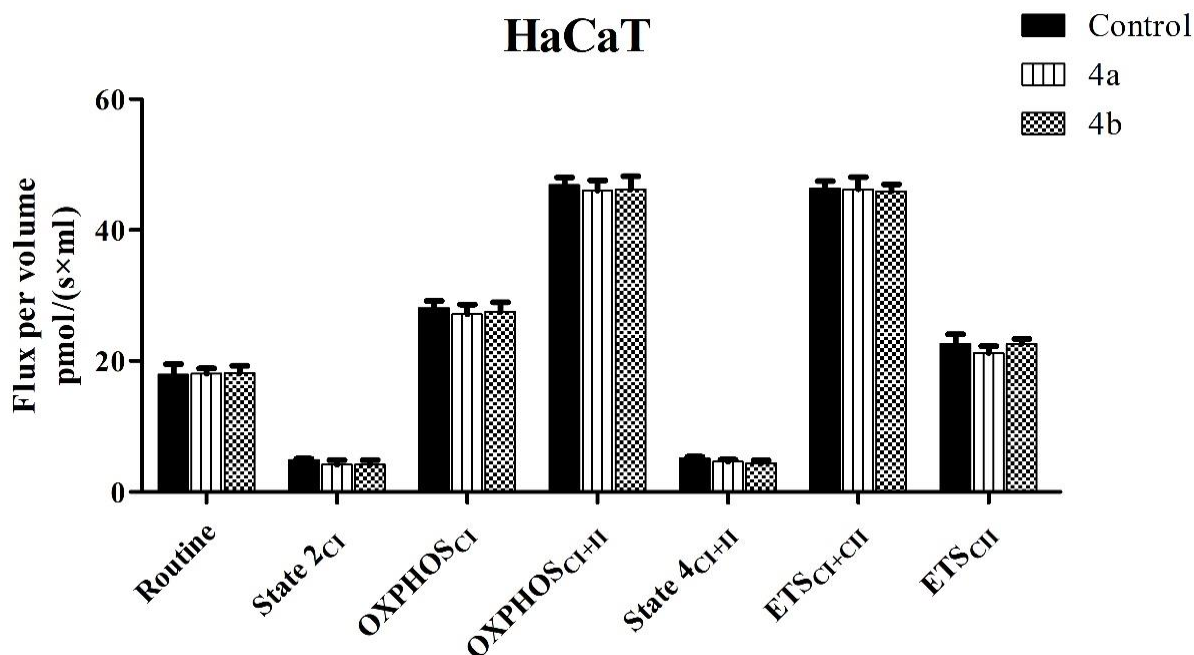


Figure 7. Rates of mitochondrial respiration measured in permeabilized HaCaT cells after treatment with compounds **4a** and **4b** (tested at IC_{50} : 18.8 μ M and IC_{50} : 20.7 μ M) for 48 h. All experiments were repeated five times and the results are reported as mean values \pm SD. One-way ANOVA followed by Bonferroni's post-test were used in order to identify statistical differences vs. control ($p > 0.05$ implies no significant differences).

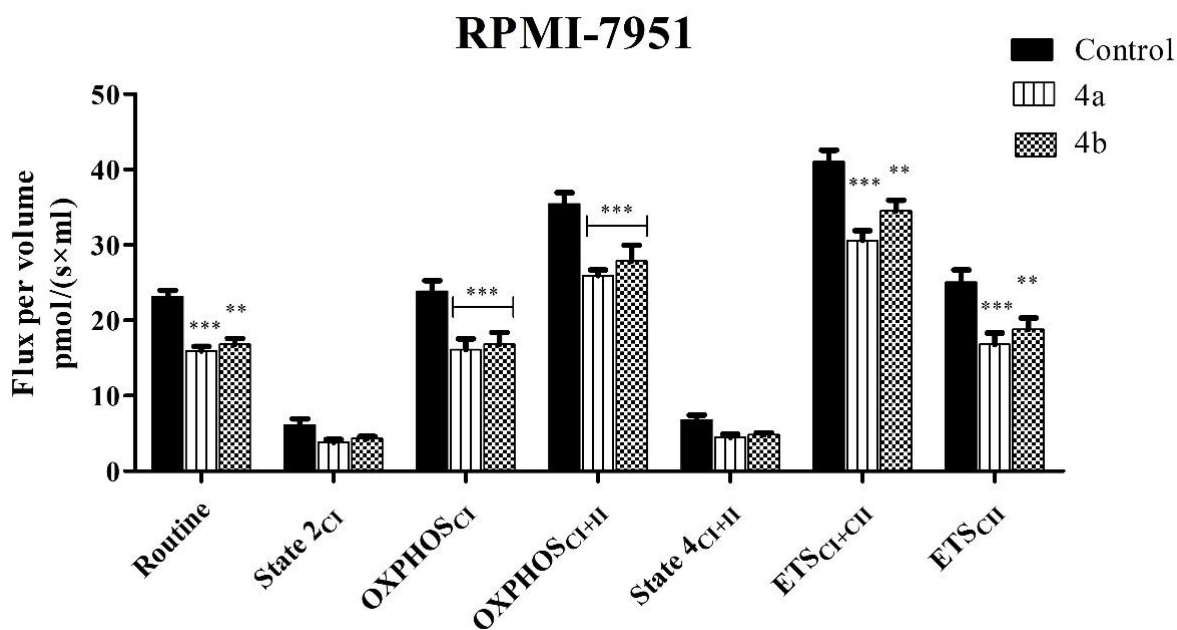


Figure 8. The rates of mitochondrial respiration in permeabilized RPMI-7951 cells after treatment with compounds **4a** and **4b** (tested at IC_{50} : 18.8 μ M and IC_{50} : 20.7 μ M, respectively) for 48 h. All experiments were repeated five times and the results are reported as mean values \pm SD. One-way ANOVA followed by Bonferroni's post-test were used in order to identify statistical differences vs. control (** $p < 0.01$ and *** $p < 0.001$).

Table 2. Mitochondrial respiratory rates of RPMI–9751 cells treated with compounds **4a** and **4b**.

	RPMI–7951		
	Control	4a	4b
Routine	22.95	15.947	16.79
State 2CI	6.28	3.82	4.30
OXPHOSCI	24.22	15.96	16.83
OXPHOSCI + II	34.71	25.92	26.85
State 4CI + II	6.35	4.47	4.81
ETSCI + CII	42.08	30.52	31.36
ETSCII	24.87	16.49	17.83

2.6. Irritative Potential of BA Triazole Derivatives

The HET–CAM assay was involved in assessing the toxicological potential of compounds **4a–4b**. As presented in Figure 9, the investigated compounds did not interfere with the circulation process and did not produce any impairment on the vascular plexus.

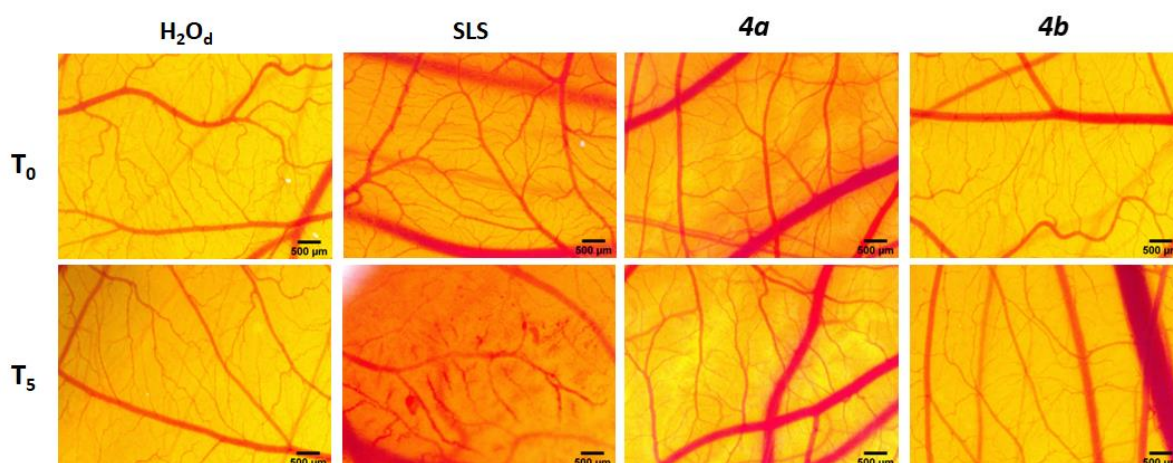


Figure 9. The irritation assessment using the HET–CAM method. Stereomicroscope images of the chorioallantoic membrane were taken before (T_0) and 300 s (T_5) after treatment with 300 μ L compounds **4a** and **4b**, respectively (tested at IC_{50} : 18.8 μ M and IC_{50} : 20.7 μ M); distilled water was used as negative control while SLS 0.5% acted as positive control). Scale bars represent 500 μ m.

The irritation potential was assessed on the Luepke scale that assigned scores between 0 and 21 according to the severity of the reaction as follows: non-irritant compounds classified between 0 and 0.9, a slight irritation was indicated by 1–4.9 values, 5–8.9 ranging values depicted moderate irritation, while strongly irritant compounds reached 9–21 values [19]. As presented in Table 3, the tested compounds did not show any irritation potential, and therefore, were suitable for mucosal and cutaneous use. These findings were noteworthy because pentacyclic triterpenes and their derivatives were known to be active in wound healing and re-epithelization. Compounds with no irritative potential, such as the BA structurally related triterpene, betulin, were currently being studied as topical formulations in phase III clinical trials for their accelerated re-epithelization effects and efficacy against epidermolysis bullosa [20,21].

Table 3. The irritation potential of tested compounds.

Compound Name	Irritation Score	Effect
H ₂ O _d	0	Non-irritant
SLS	15.3	Strong irritant
4a	0	Non-irritant
4b	0	Non-irritant

3. Discussions

Lately, a huge amount of interest has been raised by the potent and targeted antitumor effect of betulinic acid, a phytocompound identified by Pisha et al. in 1995 as an anti-melanoma agent [22]. The precise underlying mechanisms have yet to be fully understood, although many possibilities have been proposed, including various signaling pathways involved in mitochondrial apoptotic death [23]. During research, poor water solubility and, subsequently, low bioavailability were revealed as the main flaws that hampered the therapeutic use of betulinic acid as an anticancer agent. There were multiple possibilities to improve the phytocompound's aqueous solubility, including structural modifications, which may simultaneously improve the overall antitumor efficacy [6].

The triazole moiety was involved in numerous functionalizations due to its polar character, as well as its ability to form non-covalent interactions with targeted ligands, thus exhibiting pharmacophore properties. However, the introduction of a triazole moiety at C₃₀ in BA's molecule was only performed twice: by Shi et al. and Sidova et al. [9,10], by applying click chemistry on betulinic acid's C₃₀-bromo derivatives; both groups used the 1,2,3-triazole moiety. As far as we are aware, C₃₀-1,2,4-triazole derivatives were only developed by our group, using the unsubstituted triazole as a reaction partner for the brominated betulinic acid [13]. The resulted derivative revealed antitumor effects against melanoma cells exerted through apoptotic mechanisms.

Continuing our research, we tried to develop betulinic acid derivatives using aryl substituted-triazole moieties. The cytotoxic activities of both derivatives, as well as their parent compounds were tested by means of MTT assay, in order to quantitatively assess the change in cytotoxicity, induced by the chemical modulations, against various cancer cells. In our current study, we used a 50 µM threshold for IC₅₀ values, above which we considered the cytotoxicity of any particular compound to be insignificant. In all tested settings, the starting triazoles (**3a–b**) did not exhibit IC₅₀ values less than 50 µM. This is consistent with previous findings by our group on melanoma and colorectal cancer cell lines using structurally similar 1,2,4-triazole-3-derivatives [14,24], where the most active 1,2,4-triazole derivative exhibited an IC₅₀ value 149.25 µM. Meanwhile, both BA-triazole derivatives (**4a–b**) increased cytotoxicity in all tested malignant cells, except for HT-29 cells, where the 30-brominated BA derivative was slightly more active. The RPMI melanoma cell line was the most affected by compound **4a** and **4b**'s induced cytotoxic properties. These effects seem to be triggered by the presence of the triazole moiety that also revealed cytotoxic activity but to a lesser extent; therefore, we may assume that the triazole ring was included in the pharmacophore constellation of atoms in the molecule of betulinic acid. These results were supported by Sidova et al. who reported that the modification of the C₃₀ position combined with the presence of an aromatic substituent on the triazole group was part of the pharmacophore being responsible for the compounds' cytotoxicity [10]. In this case, a 1,2,3-triazole – BA derivative with a *p*-dimethylamino-phenyl substituent on the triazole ring exhibited a highly similar cytotoxic behavior to our compound **4b** against colon and lung cancer cell lines. The compound had an IC₅₀ of 26.6 µM against the A549 cell line and 32.9 µM against HCT116 cells. Furthermore, when tested in colon cancer cells, the 3-acetyl-30-brominated BA revealed a higher cytotoxicity (IC₅₀ = 15.9 µM) than most other 1,2,3-triazole derivatives, similar to our case, where the same compound (**2**) acted in a similar manner (IC₅₀ = 15.9 µM) [10]. In addition, the presence of an acetyl group at C₃

provided the molecule with the necessary degree of lipophilicity to be able to penetrate cell membranes and exert their biological effects; the above-cited study revealed that hydroxyl groups may interfere with membrane permeability due to their hydrophilicity. Similarly, Shi et al. revealed that, within C₃₀-triazole substitutions, the cytotoxic activity was favored by the presence of large side chains with lipophilic or aromatic fragments, their antiproliferative effects being stronger than those reported for betulinic acid [9]. The introduction of triazole moieties in other positions on the triterpenic scaffold also produced improved cytotoxicity; as such, ursane and lupane triazole-hybrids obtained by the functionalization of the C₂₈ carboxyl were identified as effective antitumor agents with IC₅₀ values comparable to doxorubicin, while the supplementary C₃-acetyl substituent further increased the cytotoxic effect, the respective derivatives becoming more cytotoxic than doxorubicin [25]. Unfortunately, no other triazole derivatives of betulinic acid, other than the ones mentioned above, had been evaluated against human melanoma in the literature. Given that the triazole moiety was highly likely to enhance the compound's cytotoxicity, the lupane core structure of BA may have been responsible for the slightly increased cytotoxic activity against melanoma. This was consistent with previous findings according to which betulinic acid had similar or slightly higher antimelanoma efficacy versus its activity against various types of colon or lung cancer [26]. For example, data from two studies demonstrated that the IC₅₀ values for BA against various types of colorectal and lung cancers ranged between 6.1–12.3 µg/mL for lung cancers and 3.8–16.4 µg/mL for colon cancers, while BA showed slightly lower IC₅₀ values (1.5–1.6 µg/mL) against melanoma. BA exhibited the same cytotoxic activity against H460 non-small lung cancer cells (IC₅₀ = 1.5 µg/mL) under the same environment [27,28]. With these considerations, we may state that the newly synthesized 1,2,4-triazole compounds were an effective anticancer, especially the antimelanoma agents, owing to their activity both to the triterpene scaffold and the new triazole substitution; their activity was also improved by the presence of the C₃-acetyl moiety that contributed to an adequate membrane penetration.

Keratinocytes are primary cells found in human epidermis that play a role in skin inflammatory response; the immortalized human keratinocytes HaCaT cells were established as the skin model since they do not alter the keratinocyte function [29], cellular responses, or differentiation capacity. Moreover, monolayer HaCaT cell cultures are currently used to test cellular toxicity and to conduct in vitro wound healing analysis [30]. In HaCaT cells, neither compounds **4a–b** nor their intermediates have IC₅₀ values less than 50 µM, indicating no increased cytotoxicity. The C₂₈-benzotriazole esters of the three triterpenic acids showed similar outcomes, with all compounds exhibiting high levels of antitumor selectivity [31].

Very early studies on betulinic acid's antitumor mechanisms revealed its capacity to induce mitochondrial apoptosis [32]; many of its derivatives also revealed pro-apoptotic properties [33–35]. Therefore, we hypothesized that the BA triazole derivatives **4a** and **4b** synthesized in the current study, will act by similar mechanisms; subsequently, DAPI staining revealed apoptotic signs in all treated cancer cells. To further validate DAPI results, RPMI-7951 melanoma cells were subjected to quantitative real-time PCR in order to assess the variations in Bcl-2 and BAX gene expressions. Both compounds induced the upregulation of BAX accompanied by the downregulation of Bcl-2 genes, thus showing a clear pro-apoptotic activity. These results were consistent with similar reports regarding the parent structure, where BA was revealed as a strong inhibitor of several signaling pathways, being capable of selective apoptosis induction [36]. A novel triazole derivative of BA induced the scindation of Bcl-2 combined with BAX translocation, finally resulting in a decreased Bcl-2/BAX ratio in leukemia cells [37]. Our own research group already obtained C₂₈-triazole-substituted compounds starting from betulinic acid that acted in a similar manner on the Bcl-2/BAX ratio [31]; in addition, the C₃₀-triazole derivative of BA synthesized by our group [13] also revealed similar results, certifying for the first time that such compounds were able to induce apoptosis. Therefore, our findings were consistent with these previously published data and, due to similar structures to the above-mentioned

triazole derivatives, we may assume that the currently reported compounds also caused the disruption of mitochondrial membrane potential.

Subsequently, the mitochondrial function was evaluated through high respirometry after the treatment of both malignant melanoma and normal cells with compounds **4a** and **4b**; the results revealed the inhibition of mitochondrial respiration in RPMI–7951 cells, while normal HaCaT cells mitochondrial respiration remained unaffected. These results were consistent with previous data that reported a decreased mitochondrial activity in A375 melanoma cells for betulinic acid alone; BA considerably reduced all respiratory parameters: routine, baseline, active, leak, and maximum uncoupled respiration [38]. A similar effect in terms of mitochondrial respiration was observed when benzotriazole esters of triterpenic acids were tested against the A375 melanoma cell line; all tested compounds were able to inhibit respiratory rates thus causing mitochondrial dysfunction and cell death [31]. As previously stated, mitochondrial malfunction and ATP production impairment had a beneficial impact in cancer cells, and any drugs that may have generated such alterations at the mitochondrial level could be regarded as prospective cancer therapy approaches.

The HET–CAM assay assessed the irritation potency and toxicity of **4a** and **4b**, which did not interfere with the circulation process and did not produce any impairment on the vascular plexus. The application of CAM assay was an easy way to study intact tissues including capillaries, arteries, and veins; various chemicals may have come in direct contact with CAM, triggering inflammatory reactions such as: hemorrhage, lysis, and coagulation. The test was a reliable opportunity to predict the irritant character of given compounds and could select irritating and non–irritating substances [39]. According to the Luepke score, the tested compounds did not show any irritation potential, and therefore, were suitable for mucosal and cutaneous use.

4. Materials and Methods

4.1. Reagents

All reagents for both chemical and biological procedures were purchased from Sigma Aldrich (Merck KGaA, Darmstadt, Germany) and further used without additional purification.

4.2. Chemistry

4.2.1. Instruments

The NMR spectrometry was conducted by using a Bruker NEO 400 MHz Spectrometer configured with a 5 mm QNP direct detection probe with z–gradients. All spectra were registered within standard parameters in DMSO–*d*₆ or CDCl₃ and calibrated on the solvent residual peak (1H: 2.51 ppm for DMSO–*d*₆ or 7.26 ppm for CDCl₃; ¹³C: 39.5 ppm for DMSO–*d*₆ or 77.0 for CDCl₃). Melting points were recorded on a Biobase melting point instrument (Biobase Group, Shandong, China); thin–layer chromatography was conducted on 60 F254 silica gel–coated plates (Merck KGaA, Darmstadt, Germany). LC/MS spectra were recorded by using methanolic solutions on an Agilent 6120 Quadrupole LC/MS system (Santa Clara, CA, USA) equipped with a UV detector, an ESI ionization source and a Zorbax Rapid Resolution SB–C18 (1.8 μm; 50 2.1 mm) column in the negative ion mode; the samples were analysed at 0.4 mL/min, 25 °C, and *l* = 250 nm. The mobile phase contained a 1 mM isocratic combination of 85% methanol with 15% ammonium formate.

4.2.2. General Synthesis for 5–Substituted–1H–1,2,4–Triazole–3–Thiols

The synthesis of 5–R–1,2,4–triazole–3–thiol was accomplished according to previously published protocols [14]. A total of 20 mmoles of thiosemicarbazide were dissolved in 50 mL DMF under magnetic stirring, followed by the addition of 22 mmoles pyridine and 20 mmoles aryl chloride. Magnetic stirring was continued at room temperature for 30 min before the temperature was raised to 50 °C and maintained for approximately 1 h; the end-point of the reaction was validated by TLC. The resulting aryl–thiosemicarbazides were precipitated with aqueous HCl, filtered, and dried. 5–substituted–1H–1,2,4–triazole–3–thiols were obtained by cyclizing 10 mmoles of obtained aryl–thiosemicarbazide in ethano-

lic NaOH at reflux, until TLC control indicated the end of the reaction. The resulting 5-substituted-1H-1,2,4-triazole-3-thiols were precipitated using HCl.

5-(4-methoxyphenyl)-1H-1,2,4-triazole-3-thiol (**3a**); white powder, m.p. 234–237 °C (uncorrected), yield 60%; ¹H NMR (400.13 MHz, DMSO-*d*₆, δ, ppm): 13.70 (s, 1H), 13.56 (s, 1H), 7.85 (d, *J* = 8.6 Hz, 2H), 7.07 (d, *J* = 8.6 Hz, 2H), 3.81 (s, 3H); ¹³C NMR (100.6 MHz, DMSO-*d*₆, δ, ppm): 165.6, 161.0, 150.1, 127.3, 117.8, 114.5, 55.4. LC-MS Rt = 0.427 min, *m/z* = 206 [M-H]⁺–.

5-[4-(dimethylamino)phenyl]-1H-1,2,4-triazole-3-thiol (**3b**); white powder, m.p. 282–287 °C (uncorrected), yield 70%; ¹H NMR (400.13 MHz, DMSO-*d*₆, δ, ppm): 13.39 (br s, 2H), 7.72 (d, *J* = 8.9 Hz, 2H), 6.76 (d, *J* = 8.9 Hz, 2H), 2.96 (s, 6H); ¹³C NMR (100.6 MHz, DMSO-*d*₆, δ, ppm): 165.1, 151.4, 150.9, 126.7, 112.4, 111.7, 39.7 (overlapped with the residual solvent peak). LC-MS Rt = 0.49 min, *m/z* = 219 [M-H]⁺–.

4.2.3. Synthesis Procedure for 3β-O-Acetyl-30-Bromobetulinic Acid

BA was subjected to acetylation according to the modified version of the procedure previously described by Petrenko et al. [15], which involved the reaction between **1** (1 Eq) and acetic anhydride (4 Eq) in a medium of pyridine, while also adding DMAP (0.1 Eq); the mixture was stirred for 12 h at room temperature. The resulting mixture was initially diluted with water and further extracted with CHCl₃. Anhydrous MgSO₄ was used to dry the organic phase, followed by the removal of the remaining solvent in a rotary evaporator. Afterward, 1.78 g of recently recrystallized NBS (10 mmoles) was added to 2.5 g of 3-O-Acetyl-betulinic acid (5 mmoles) that had been solubilized in 50 mL CCl₄. The reaction continued under stirring for 48 h at room temperature followed by filtration, solvent removal, and chromatographic separation over silica using a 40:1 volume ratio of CHCl₃ and ethyl acetate. The spectral data collected for 3β-O-Acetyl-30-bromobetulinic acid were reported by our group in a previously published paper [13] and were aligned with the existing literature [10].

4.2.4. General Synthesis for 30-Triazole Substituted BA Derivatives

In total 5 mL DMF were added to 0.3 mmoles anhydrous K₂CO₃ and 0.2 mmoles 3β-O-Acetyl-30-bromobetulinic acid and magnetically stirred for 10 min at 25 °C; after the addition of 0.2 mmoles 5-R-1H-1,2,4-triazole-3-thiol, the mixture continued to be stirred for another 72 h at 25 °C. In the next step, 50 mL of water were added to the mixture, which was then extracted with CHCl₃ (4 × 15 mL). The organic phase was dried using anhydrous MgSO₄, the solvent was removed, and the crude product was then chromatographed using 2:1 CHCl₃: ethyl acetate (*v/v*).

3β-O-Acetyl-30-[5-(4-methoxyphenyl)-1H-1,2,4-triazol-3-yl]-sulfanyl-betulinic acid (**4a**); white crystalline powder, yield 22%; ¹H NMR (400.13 MHz, CDCl₃, δ, ppm): 8.01 (d, *J* = 8.5 Hz, 2H), 6.84 (d, *J* = 8.8 Hz, 2H), 5.09 (s, 1H), 4.97 (s, 1H), 4.44 (dd, *J* = 6.0 Hz, *J* = 9.6 Hz, 1H), 3.91 (AB spin system, *J* = 14.0 Hz, 2H), 3.82 (s, 3H), 3.01 (td, *J* = 4.3 Hz, *J* = 11.3 Hz, 1H), 2.28 (d, *J* = 11.9 Hz, 1H), 2.17–2.09 (m, 2H), 2.04 (s, 3H), 1.92 (dd, *J* = 8.2 Hz, *J* = 12.9 Hz, 1H), 1.72 (t, *J* = 11.1 Hz, 1H), 1.57–1.14 (m, 15H), 0.97–0.72 (m, 21H); ¹³C NMR (100.6 MHz, CDCl₃, δ, ppm): 180.8, 171.3, 161.9, 155.9, 155.8, 149.5, 128.7, 128.4, 114.5, 112.2, 81.1, 56.3, 55.4, 50.7, 50.3, 43.8, 42.4, 40.7, 38.3, 37.8, 37.1, 36.8, 34.2, 32.7, 32.0, 29.7, 27.9, 27.0, 23.7, 21.4, 21.0, 18.2, 16.5, 16.2, 16.0, 14.7. LC-MS Rt = 1.85 min, *m/z* = 703 [M-H]⁺–.

3β-O-Acetyl-30-[5-[4-(dimethylamino)phenyl]-1H-1,2,4-triazol-3-yl]sulfanyl-betulinic acid (**4b**); pale yellow crystalline powder, yield 25%; ¹H NMR (400.13 MHz, CDCl₃, δ, ppm): 7.86 (d, *J* = 8.7 Hz, 2H), 6.73 (d, *J* = 8.1 Hz, 2H), 5.08 (s, 1H), 4.96 (s, 1H), 4.44 (dd, *J* = 5.9 Hz, *J* = 9.8 Hz, 1H), 3.87 (s, 2H), 3.02–2.99 (m, 7H), 2.28 (d, *J* = 12.0 Hz, 1H), 2.20–2.10 (m, 2H), 2.04 (s, 3H), 1.93 (dd, *J* = 7.8 Hz, *J* = 13.1 Hz, 1H), 1.72 (t, *J* = 11.2 Hz, 1H), 1.57–1.00 (m, 15H), 0.94–0.73 (m, 21H); ¹³C NMR (100.6 MHz, CDCl₃, δ, ppm): 180.7, 171.2, 157.7, 157.3, 151.4, 149.9, 129.0, 128.0, 112.3, 111.7, 81.1, 56.4, 55.4, 50.6, 50.3, 44.0, 43.5, 42.4, 40.7, 40.5, 38.3, 37.8, 37.1, 36.9, 34.2, 32.6, 32.1, 29.7, 27.9, 26.9, 23.7, 21.4, 21.0, 18.2, 16.5, 16.2, 16.0, 14.7. LC-MS Rt = 1.97 min, *m/z* = 716 [M-H]⁺–.

4.3. Cell Culture

Immortalized human keratinocytes HaCaT (CLS Cell Lines Service GmbH, Eppelheim, Germany), human malignant melanoma RPMI–7951, human colorectal adenocarcinoma HT–29, and human lung carcinoma A549 (ATCC[®] HTB–66[™], HTB–38[™], and CCL–185[™], American Type Culture Collection ATCC, Lomianki, Poland) cell lines were selected for this study. DMEM, EMEM, McCoy's 5A Medium, and F–12K Medium (Kaighn's Modification of Ham's F–12 Medium), respectively, were used to culture BaCaT, RPMI–7951, HT–29, and A549 cells; 10% FBS and 1% penicillin/streptomycin mixture (10,000 IU/mL) were added to all media. All experimental procedures were conducted under standard conditions consisting in incubation at 37 °C under 5% CO₂ atmosphere.

4.4. Cellular Viability

The 3–(4,5–dimethylthiazol–2–yl)–2,5–diphenyltetrazolium bromide (MTT) was used to assess cell viability. Briefly, the different types of cells were seeded in 96–well plates (1×10^4 cells/well) followed by stimulation with 0.08, 0.4, 2, 10, 25, and 50 μ M of the tested compounds (**1–4b**) previously solubilized in 0.5% DMSO. An amount of 10 μ L/well MTT reagent were added to the plates after a 48 h stimulation period; the plates were then maintained at 37 °C for 3 h, followed by the addition of solubilization buffer (100 μ L/well). The absorbance values were read at 570 nm using a xMark[™] Microplate Spectrophotometer, Bio–Rad. All experiments were conducted in triplicate allowing for the presentation of data as mean values \pm SD.

4.5. Immunofluorescence Assay

The 4, 6'–Diamidino–2–Phenylindole (DAPI) staining was used to assess the indicative signs of apoptosis; briefly, RPMI–7951 cells (1×10^6 cells/well) were stimulated for 48 h with tested compounds (**4a**, **4b**) using concentrations matching their respective IC₅₀ values. Cells were fixated with 4% paraformaldehyde, permeabilized with 2% Triton X–100 in PBS and then washed 3 times with cold PBS, the cells were blocked for 1 h at 25 °C using 30% FCS in 0.01% Triton X. In the final step, the cells were treated with 300 nM DAPI and microscopically assessed by using the Olympus IX73 inverted microscope (Olympus, Tokyo, Japan) equipped with CellSens V1.15 software.

4.6. Mitochondrial Respiration Assessment

Mitochondrial respiration was evaluated at 37 °C by high resolution respirometry (HRR, Oxygraph–2k Oroboros Instruments GmbH, Innsbruck, Austria) using a previously described modified substrate uncoupler–inhibitor titration (SUIT) protocol [40]. Malignant cells (RPMI–7951, HT–29, A549) were cultured until reaching 80–85% confluence and treated for 48 h with compounds **4a** and **4b** (at their respective IC₅₀ values). Cells were then washed with PBS, trypsinized, counted, and resuspended (1×10^6 /mL cells) in mitochondrial respiration medium (MIRO5: EGTA 0.5 mM, taurine 20 mM, K–lactobionate 60 mM, MgCl₂ 10 mM, D–sucrose 110 mM, HEPES 20 mM, 3mM KH₂PO₄, and BSA 1 g/l, pH 7.1). Cells were introduced in the respirometric device in the presence of MIRO5 and maintained under the oxygen flux for 15 min when routine respiration was recorded followed by basal respiration (State2_{CI}), after the addition of digitonine (35 μ g/ 1×10^6 cells, a cell membrane permeabilizer) and CI substrates: glutamate (10 mM) and malate (5 mM).

The addition of ADP (5 mM) allowed for the measurement of the active respiration reliant on CI (OXPHOSCI), and the addition of succinate (10 mM), a CII substrate, allowed for the measurement of the active respiration reliant on both CI and CII (OXPHOSCI + CII). The assessment of LEAK respiration dependent on CI and CII (State4_{CI} + II) was enabled by the consecutive suppression of complex V with oligomycin (1 g/mL). Subsequently, successive titrations with *p*–(trifluoromethoxy) phenylhydrazone carbonyl cyanide – FCCP (1 M/step) led to the measurement of the maximal respiratory capacity of the electron transport system (ETSCI + II), whereas the addition of rotenone (0.5 M, a CI inhibitor) ensured the measurement of the maximal respiratory capacity of the ETS that was

dependent solely on CI (ETSCI). In the last phase of the process, mitochondrial respiration was suppressed by adding antimycin A (2.5 M), a CIII inhibitor, and residual oxygen consumption was then measured (ROX) and used to adjust all acquired values.

4.7. Quantitative Real–Time PCR

RPMI–795 cells were treated with compounds **4a** and **4b** (at their respective IC₅₀ value) for 48 h. The Quick–RNA™ purification kit (Zymo Research Europe, Freiburg im Breisgau, Germany) and the TRIzol reagent (Thermo Fisher Scientific, Inc., Waltham, MA, USA) were used to isolate the total RNA. Total RNA transcription was conducted using a Maxima® First Strand cDNA Synthesis Kit (Thermo Fisher Scientific, Inc., Waltham, MA, USA). Quant Studio 5 real–time PCR system (Thermo Fisher Scientific, Inc., Waltham, MA, USA) was used to conduct the quantitative real–time PCR analysis, in the presence of Power SYBR–Green PCR Master Mix (Thermo Fisher Scientific, Inc.). The primer pairs used were acquired from Thermo Fisher Scientific Inc. (Waltham, MA, USA) and were as follows: 18 S (forward: 5′GTAACCCGTTGAACCCATT3′ and reverse: 5′CCA–TCC–AAT–CGG–TAGTAG–CG3′), BAX (forward: 5′GGCCGGTTGTCGCCCTTTT3′ and reverse: 5′CCGCTCCCGGAGGAAGTCCA3′) and Bcl–2 (forward: 5′CGGGAGATGTCGCCCTGGT3′ and reverse: 5′–GCATGCTGGGGCCGTACAGT–3′). Normalized, relative expression data were calculated using the comparative threshold cycle (2^{–ΔΔCt}) method.

4.8. Evaluation of Compounds **4a**, **4b** Irritation Potential Using the HET–CAM Assay

The HET–CAM *in vivo* protocol was applied in order to assess the safety profile for use in living tissues; the protocol involved using the developing chorioallantoic membrane in embryonated chicken (*Gallus domesticus*) eggs and followed the ICCVAM recommendations [41] tailored to our own circumstances. According to a modified version of the conventional methodology [42], the eggs were incubated at 37 °C and 50% humidity. On the third day of incubation, 5–6 mL of albumen was extracted, followed by the construction of a hole in the top of the eggs. On the developing chorioallantoic membrane of the chick embryo, 300 μL of both the control and test chemicals **4a** and **4b** were administered at their respective IC₅₀ values. The CAM alterations were monitored using stereomicroscopy (Discovery 8 Stereomicroscope, Zeiss), recording significant pictures (Axio CAM 105 color, Zeiss) before the application and after five minutes of contact with the materials. During the 5 min, the effect on three parameters, namely hemorrhage, lysis, and coagulability of the vascular plexus, was detected. Every experiment was conducted in triplicate. The results were expressed as irritation factor values, calculated using the given formula, and compared to distillate water as a negative control and SLS 0.5% as a positive control with an IF of 15.3 (according to the Luepke scale: 0–0.9 non–irritant, 1–4.9 weak irritant, 5–8.9 moderate irritant, and 9–21 strong irritant [19]).

$$IS = 5 \times \frac{301 - \text{Sec H}}{300} + 7 \times \frac{301 - \text{Sec L}}{300} + 9 \times \frac{301 - \text{Sec C}}{300}$$

where H = hemorrhage; L = vascular lysis; C = coagulation; Sec H = start of hemorrhage reactions (s); Sec L = onset of vessel lysis on CAM (s); Sec C = onset of (s).

4.9. Statistical Analysis

The statistical differences vs. control of the cellular viability and quantitative rtPCR results were determined using one–way ANOVA analysis followed by Dunnett post–test. For the high–resolution respirometry studies, the statistical differences vs. control of mitochondrial respiratory rates were determined using two–way ANOVA analysis followed by Bonferroni’s multiple comparisons post–test (GraphPad Prism version 6.0.0, GraphPad Software, San Diego, CA, USA). The difference between groups was considered statistically significant if $p < 0.05$ and was marked with * ($p < 0.05$), ** ($p < 0.01$), and *** ($p < 0.001$). The IC₅₀ values were calculated using the GraphPad Prism software (San Diego, CA, USA).

5. Conclusions

The current paper described the synthesis and cytotoxicity investigation of two novel aryl substituted-1,2,4-triazole derivatives of betulinic acid against RPMI-7951 (human malignant melanoma), HT-29 (human colorectal adenocarcinoma), A549 (human lung carcinoma), as well as healthy human keratinocytes HaCaT cell line. Among all cell lines subjected to cytotoxicity screening, the two compounds were proven to induce the highest cytotoxic effects against melanoma cells (IC₅₀: 18.8 µM for 4a and 20.7 µM for 4b) and were more cytotoxically active than their parent compounds as well. Both derivatives also induced apoptotic related nuclear changes, induced a pro-apoptotic fold change expression in the Bcl-2/BAX gene ratio, and impaired mitochondrial function. While the antiproliferative biological evaluation indicated that C₃₀ substitution using 1,2,4-triazole was highly advantageous for the overall antiproliferative potential, especially against melanoma, the synthetic procedure needs future adjustments in order to produce higher yields. Nonetheless, BA-1,2,4-triazole derivatives stand as promising scaffolds for the development of novel heterocyclic triterpenoids with antimelanoma activity.

Supplementary Materials: The following supporting information can be downloaded at: <https://www.mdpi.com/article/10.3390/pr11010101/s1>. Figure S1: ¹H NMR spectra of compound 2; Figure S2: ¹³C NMR spectra of compound 2; Figure S3: ¹H NMR spectra of compound 3a; Figure S4: ¹³C NMR spectra of compound 3a; Figure S5: ¹H NMR spectra of compound 3b; Figure S6: ¹³C NMR spectra of compound 3b; Figure S7: ¹H NMR spectra of compound 4a; Figure S8: ¹³C NMR spectra of compound 4a; Figure S9: ¹H NMR spectra of compound 4b; Figure S10: ¹³C NMR spectra of compound 4b.

Author Contributions: Conceptualization: G.N. and M.M.; methodology: G.N., M.M., A.M. (Alexandra Mioc), M.B.-P., R.R., R.G., A.M. (Andreea Milan), A.P., Ş.A., A.S., C.D. and C.Ş.; validation: A.M. (Alexandra Mioc) and M.M.; investigation: G.N. and M.M.; writing—original draft preparation: G.N., M.M., A.M. (Alexandra Mioc), M.B.-P., R.R., R.G., A.M. (Andreea Milan), A.P., Ş.A., A.S. and C.D.; writing—review and editing: C.Ş.; visualization: G.N., R.R. and R.G.; supervision: M.M. and C.Ş.; project administration: M.M. and C.Ş.; funding acquisition: M.M. and C.Ş. All authors have read and agreed to the published version of the manuscript.

Funding: This research was funded by the Romanian UEFISCDI national grant PN-III-P1-1.1-PD-2019-1078 (M.M.) and an Internal grant at “Victor Babes” University of Medicine and Pharmacy, Grant 1EXP/1233/30.01.2020 LUPSKINPATH (C.Ş.).

Institutional Review Board Statement: Not applicable.

Informed Consent Statement: Not applicable.

Data Availability Statement: Data is contained within the article and Supplementary Files.

Conflicts of Interest: The authors declare no conflict of interest.

References

1. Amjad, M.T.; Chidharla, A.; Kasi, A. *Cancer Chemotherapy*; StatPearls Publishing: Tampa, FL, USA, 2022.
2. Schirmmacher, V. From Chemotherapy to Biological Therapy: A Review of Novel Concepts to Reduce the Side Effects of Systemic Cancer Treatment (Review). *Int. J. Oncol.* **2019**, *54*, 407–419. [[CrossRef](#)]
3. Dehelean, C.A.; Marcovici, I.; Soica, C.; Mioc, M.; Coricovac, D.; Iurciuc, S.; Cretu, O.M.; Pinzaru, I. Plant-Derived Anticancer Compounds as New Perspectives in Drug Discovery and Alternative Therapy. *Molecules* **2021**, *26*, 1109. [[CrossRef](#)]
4. Ghante, M.H.; Jamkhande, P.G. Role of Pentacyclic Triterpenoids in Chemoprevention and Anticancer Treatment: An Overview on Targets and Underling Mechanisms. *J. Pharmacopunct.* **2019**, *22*, 55–67. [[CrossRef](#)]
5. Lou, H.; Li, H.; Zhang, S.; Lu, H.; Chen, Q. A Review on Preparation of Betulinic Acid and Its Biological Activities. *Molecules* **2021**, *26*, 5583. [[CrossRef](#)]
6. Zhong, Y.; Liang, N.; Liu, Y.; Cheng, M.-S. Recent Progress on Betulinic Acid and Its Derivatives as Antitumor Agents: A Mini Review. *Chin. J. Nat. Med.* **2021**, *19*, 641–647. [[CrossRef](#)]
7. Kerru, N.; Gummidi, L.; Maddila, S.; Gangu, K.K.; Jonnalagadda, S.B. A Review on Recent Advances in Nitrogen-Containing Molecules and Their Biological Applications. *Molecules* **2020**, *25*, 1909. [[CrossRef](#)]

8. Majeed, R.; Sangwan, P.L.; Chinthakindi, P.K.; Khan, I.; Dangroo, N.A.; Thota, N.; Hamid, A.; Sharma, P.R.; Saxena, A.K.; Koul, S. Synthesis of 3-O-Propargylated Betulinic Acid and Its 1,2,3-Triazoles as Potential Apoptotic Agents. *Eur. J. Med. Chem.* **2013**, *63*, 782–792. [[CrossRef](#)]
9. Shi, W.; Tang, N.; Yan, W.D. Synthesis and Cytotoxicity of Triterpenoids Derived from Betulin and Betulinic Acid via Click Chemistry. *J. Asian Nat. Prod. Res.* **2015**, *17*, 159–169. [[CrossRef](#)]
10. Sidova, V.; Zoufaly, P.; Pokorny, J.; Dzubak, P.; Hajduch, M.; Popa, I.; Urban, M. Cytotoxic Conjugates of Betulinic Acid and Substituted Triazoles Prepared by Huisgen Cycloaddition from 30-Azidoderivatives. *PLoS ONE* **2017**, *12*, e0171621. [[CrossRef](#)]
11. Suman, P.; Patel, A.; Solano, L.; Jampana, G.; Gardner, Z.S.; Holt, C.M.; Jonnalagadda, S.C. Synthesis and Cytotoxicity of Baylis-Hillman Template Derived Betulinic Acid-Triazole Conjugates. *Tetrahedron* **2017**, *73*, 4214–4226. [[CrossRef](#)]
12. Sousa, J.L.C.; Freire, C.S.R.; Silvestre, A.J.D.; Silva, A.M.S. Recent Developments in the Functionalization of Betulinic Acid and Its Natural Analogues: A Route to New Bioactive Compounds. *Molecules* **2019**, *24*, 355. [[CrossRef](#)] [[PubMed](#)]
13. Nistor, G.; Mioc, M.; Mioc, A.; Balan-Porcarasu, M.; Racoviceanu, R.; Prodea, A.; Milan, A.; Ghiulai, R.; Semenescu, A.; Dehelean, C.; et al. The C30-Modulation of Betulinic Acid Using 1,2,4-Triazole: A Promising Strategy for Increasing Its Antimelanoma Cytotoxic Potential. *Molecules* **2022**, *27*, 7807. [[CrossRef](#)] [[PubMed](#)]
14. Mioc, M.; Soica, C.; Bercean, V.; Avram, S.; Balan-Porcarasu, M.; Coricovac, D.; Ghiulai, R.; Muntean, D.; Andrica, F.; Dehelean, C.; et al. Design, Synthesis and Pharmacotoxicological Assessment of 5-Mercapto-1,2,4-Triazole Derivatives with Antibacterial and Antiproliferative Activity. *Int. J. Oncol.* **2017**, *50*, 1175–1183. [[CrossRef](#)]
15. Petrenko, N.I.; Elantseva, N.V.; Petukhova, V.Z.; Shakirov, M.M.; Shul'ts, E.E.; Tolstikov, G.A. Synthesis of Betulonic Acid Derivatives Containing Amino-Acid Fragments. *Chem. Nat. Compd.* **2002**, *38*, 331–339. [[CrossRef](#)]
16. Chen, B.-H.; Chang, H.B. Inhibition of Lung Cancer Cells A549 and H460 by Curcuminoid Extracts and Nanoemulsions Prepared from Curcuma Longa Linnaeus. *Int. J. Nanomed.* **2015**, *10*, 5059. [[CrossRef](#)]
17. Mioc, M.; Pavel, I.Z.; Ghiulai, R.; Coricovac, D.E.; Farcaş, C.; Mihali, C.-V.; Oprean, C.; Serafim, V.; Popovici, R.A.; Dehelean, C.A.; et al. The Cytotoxic Effects of Betulin-Conjugated Gold Nanoparticles as Stable Formulations in Normal and Melanoma Cells. *Front. Pharmacol.* **2018**, *9*, 429. [[CrossRef](#)]
18. Eidet, J.R.; Pasovic, L.; Maria, R.; Jackson, C.J.; Utheim, T.P. Objective Assessment of Changes in Nuclear Morphology and Cell Distribution Following Induction of Apoptosis. *Diagn. Pathol.* **2014**, *9*, 92. [[CrossRef](#)]
19. Luepke, N.P. Hen's Egg Chorioallantoic Membrane Test for Irritation Potential. *Food Chem. Toxicol. Int. J. Publ. Br. Ind. Biol. Res. Assoc.* **1985**, *23*, 287–291. [[CrossRef](#)] [[PubMed](#)]
20. Barret, J.P.; Podmelle, F.; Lipový, B.; Rennekampff, H.-O.; Schumann, H.; Schwieger-Briel, A.; Zahn, T.R.; Metelmann, H.-R. Accelerated Re-Epithelialization of Partial-Thickness Skin Wounds by a Topical Betulin Gel: Results of a Randomized Phase III Clinical Trials Program. *Burns* **2017**, *43*, 1284–1294. [[CrossRef](#)]
21. Schwieger-Briel, A.; Ott, H.; Kiritsi, D.; Laszczyk-Lauer, M.; Bodemer, C. Mechanism of Oleogel-S10: A Triterpene Preparation for the Treatment of Epidermolysis Bullosa. *Dermatol. Ther.* **2019**, *32*, e12983. [[CrossRef](#)]
22. Pisha, E.; Chai, H.; Lee, I.-S.; Chagwedera, T.E.; Farnsworth, N.R.; Cordell, G.A.; Beecher, C.W.W.; Fong, H.H.S.; Kinghorn, A.D.; Brown, D.M.; et al. Discovery of Betulinic Acid as a Selective Inhibitor of Human Melanoma That Functions by Induction of Apoptosis. *Nat. Med.* **1995**, *1*, 1046–1051. [[CrossRef](#)] [[PubMed](#)]
23. Kumar, P.; Bhadauria, A.S.; Singh, A.K.; Saha, S. Betulinic Acid as Apoptosis Activator: Molecular Mechanisms, Mathematical Modeling and Chemical Modifications. *Life Sci.* **2018**, *209*, 24–33. [[CrossRef](#)] [[PubMed](#)]
24. Mioc, M.; Avram, S.; Bercean, V.; Kurunczi, L.; Ghiulai, R.M.; Oprean, C.; Coricovac, D.E.; Dehelean, C.; Mioc, A.; Balan-Porcarasu, M.; et al. Design, Synthesis and Biological Activity Evaluation of S-Substituted 1H-5-Mercapto-1,2,4-Triazole Derivatives as Antiproliferative Agents in Colorectal Cancer. *Front. Chem.* **2018**, *6*, 373. [[CrossRef](#)] [[PubMed](#)]
25. Alam, M.M. 1,2,3-Triazole Hybrids as Anticancer Agents: A Review. *Arch. Pharm.* **2022**, *355*, 2100158. [[CrossRef](#)]
26. Csuk, R. Betulinic Acid and Its Derivatives: A Patent Review (2008–2013). *Expert Opin. Ther. Pat.* **2014**, *24*, 913–923. [[CrossRef](#)]
27. Zuco, V.; Supino, R.; Righetti, S.C.; Cleris, L.; Marchesi, E.; Gambacorti-Passerini, C.; Formelli, F. Selective Cytotoxicity of Betulinic Acid on Tumor Cell Lines, but Not on Normal Cells. *Cancer Lett.* **2002**, *175*, 17–25. [[CrossRef](#)]
28. Kessler, J.H.; Mullauer, F.B.; de Roo, G.M.; Medema, J.P. Broad in vitro Efficacy of Plant-Derived Betulinic Acid against Cell Lines Derived from the Most Prevalent Human Cancer Types. *Cancer Lett.* **2007**, *251*, 132–145. [[CrossRef](#)]
29. Beilin, A.K.; Gurskaya, N.G.; Evtushenko, N.A.; Alpeeva, E.V.; Kosykh, A.V.; Terskikh, V.V.; Vasiliev, A.V.; Vorotelyak, E.A. Immortalization of Human Keratinocytes Using the Catalytic Subunit of Telomerase. *Dokl. Biochem. Biophys.* **2021**, *496*, 5–9. [[CrossRef](#)]
30. Şenkal, S.; Burucku, D.; Hayal, T.B.; Kiratli, B.; Şisli, H.B.; Sagraç, D.; Asutay, B.; Sumer, E.; Şahin, F.; Dogan, A. 3D Culture Of HaCaT Keratinocyte Cell Line as an in vitro Toxicity Model. *Trak. Univ. J. Nat. Sci.* **2022**, *23*, 211–220. [[CrossRef](#)]
31. Mioc, M.; Mioc, A.; Prodea, A.; Milan, A.; Balan-Porcarasu, M.; Racoviceanu, R.; Ghiulai, R.; Iovanescu, G.; Macasoi, I.; Draghici, G.; et al. Novel Triterpenic Acid—Benzotriazole Esters Act as Pro-Apoptotic Antimelanoma Agents. *Int. J. Mol. Sci.* **2022**, *23*, 9992. [[CrossRef](#)] [[PubMed](#)]
32. Fulda, S. Betulinic Acid for Cancer Treatment and Prevention. *Int. J. Mol. Sci.* **2008**, *9*, 1096–1107. [[CrossRef](#)]
33. Santos, R.C.; Salvador, J.A.R.; Cortés, R.; Pachón, G.; Marín, S.; Cascante, M. New Betulinic Acid Derivatives Induce Potent and Selective Antiproliferative Activity through Cell Cycle Arrest at the S Phase and Caspase Dependent Apoptosis in Human Cancer Cells. *Biochimie* **2011**, *93*, 1065–1075. [[CrossRef](#)] [[PubMed](#)]

34. Zhang, L.; Hou, S.; Li, B.; Pan, J.; Jiang, L.; Zhou, G.; Gu, H.; Zhao, C.; Lu, H.; Ma, F. Combination of Betulinic Acid with Diazen-1-Ium-1,2-Diolate Nitric Oxide Moiety Donating a Novel Anticancer Candidate. *Onco. Targets. Ther.* **2018**, *11*, 361–373. [[CrossRef](#)] [[PubMed](#)]
35. Nedopekina, D.A.; Gubaidullin, R.R.; Odinokov, V.N.; Maximchik, P.V.; Zhivotovsky, B.; Bel'skii, Y.P.; Khazanov, V.A.; Manuylova, A.V.; Gogvadze, V.; Spivak, A.Y. Mitochondria-Targeted Betulinic and Ursolic Acid Derivatives: Synthesis and Anticancer Activity. *Medchemcomm* **2017**, *8*, 1934–1945. [[CrossRef](#)] [[PubMed](#)]
36. Cháirez-Ramírez, M.H.; Moreno-Jiménez, M.R.; González-Laredo, R.F.; Gallegos-Infante, J.A.; Rocha-Guzmán, N.E. Lupane-Type Triterpenes and Their Anti-Cancer Activities against Most Common Malignant Tumors: A Review. *EXCLI J.* **2016**, *15*, 758–771. [[CrossRef](#)]
37. Khan, I.; Guru, S.K.; Rath, S.K.; Chinthakindi, P.K.; Singh, B.; Koul, S.; Bhushan, S.; Sangwan, P.L. A Novel Triazole Derivative of Betulinic Acid Induces Extrinsic and Intrinsic Apoptosis in Human Leukemia HL-60 Cells. *Eur. J. Med. Chem.* **2016**, *108*, 104–116. [[CrossRef](#)]
38. Coricovac, D.; Dehelean, C.A.; Pinzaru, I.; Mioc, A.; Aburel, O.-M.; Macasoi, I.; Draghici, G.A.; Petean, C.; Soica, C.; Boruga, M.; et al. Assessment of Betulinic Acid Cytotoxicity and Mitochondrial Metabolism Impairment in a Human Melanoma Cell Line. *Int. J. Mol. Sci.* **2021**, *22*, 4870. [[CrossRef](#)]
39. Budai, P.; Kormos, É.; Buda, I.; Somody, G.; Lehel, J. Comparative Evaluation of HET-CAM and ICE Methods for Objective Assessment of Ocular Irritation Caused by Selected Pesticide Products. *Toxicol. Vitro.* **2021**, *74*, 105150. [[CrossRef](#)]
40. Petrus, A.; Ratiu, C.; Noveanu, L.; Lighezan, R.; Rosca, M.; Muntean, D.; Duicu, O. Assessment of Mitochondrial Respiration in Human Platelets. *Rev. Chim.* **2017**, *68*, 768–771. [[CrossRef](#)]
41. Interagency Coordinating Committee on the Validation of Alternative Methods (ICCVAM). ICCVAM-Recommended Test Method Protocol: Hen' s Egg Test—Chorioallantoic Membrane (HET-CAM) Test Method. 2010, B30–B38. Available online: <https://ntp.niehs.nih.gov/iccvam/docs/protocols/ivocular-hetcam.pdf> (accessed on 1 October 2022).
42. Maghiari, A.L.; Coricovac, D.; Pinzaru, I.A.; Macasoi, I.G.; Marcovici, I.; Simu, S.; Navolan, D.; Dehelean, C. High Concentrations of Aspartame Induce Pro-Angiogenic Effects in Ovo and Cytotoxic Effects in HT-29 Human Colorectal Carcinoma Cells. *Nutrients* **2020**, *12*, 3600. [[CrossRef](#)]

Disclaimer/Publisher's Note: The statements, opinions and data contained in all publications are solely those of the individual author(s) and contributor(s) and not of MDPI and/or the editor(s). MDPI and/or the editor(s) disclaim responsibility for any injury to people or property resulting from any ideas, methods, instructions or products referred to in the content.